ACCEPTED VERSION

http://hdl.handle.net/2440/97738

Effects of non-carious cervical lesion size, occlusal loading and restoration on biomechanical behavior of premolar teeth

Short running title: Biomechanical behavior of premolar teeth

Lívia Fávaro Zeola[1], Fabrícia Araújo Pereira[1], Alexandre Coelho Machado[1], Bruno Rodrigues Reis[2], John Kaidonis[3], Zonghan Xie[4], Grant Townsend[3], Sarbin Ranjitkar[3], Paulo Vinícius Soares[5]

[1] Member of NCCL Research Group, Operative Dentistry and Dental Materials Department, School of Dentistry, Federal University of Uberlandia, Brazil.

[2] Member of NCCL Research Group, Professor at Health Technical School, Federal University of Uberlandia, Brazil.

[3] School of Mechanical Engineering, University of Adelaide, Australia

[4] School of Dentistry, University of Adelaide, Australia.

[5] Coordinator of NCCL Research Group, Operative Dentistry and Dental Materials Department, School of Dentistry, Federal University of Uberlandia, Brazil.

Corresponding author

Paulo Vinícius Soares, DDS, MS, PhD

NCCL Research Group - Operative Dentistry and Dental Materials Department

Av. Pará 1720, - Campus Umuarama - Bloco 4L, Sala 4L42

Uberlândia - Minas Gerais. ZIP-CODE: 38400-902 – Brazil

E-mail: paulovsoares@yahoo.com.br

Telephone number: +55 34 3225 8106

Abstract

Background: Information on fracture biomechanics has implications in materials research and clinical practice. The aim of this study was to analyze the influence of non-carious cervical lesion (NCCL) size, restorative status and direction of occlusal loading on the biomechanical behavior of mandibular premolars, using finite element analysis (FEA), strain gauge tests and fracture resistance tests.

Methods: Ten buccal cusps were loaded on the outer and inner slopes to calculate the strain generated cervically. Data were collected for healthy teeth at baseline and progressively at three lesion depths (0.5 mm, 1.0 mm and 1.5 mm), followed by restoration with resin composite. The magnitude and distribution of von Mises stress and maximum principal

stress were simulated at all stages using FEA, and fracture strength was also determined (n = 7 per group).

Results: There were significant effects of the lesion size and loading directions on stress, strain and fracture resistance (p<0.05). Fracture resistance values decreased with increase in lesion size, but returned to baseline with restorations.

Conclusions: Combined assessment of computer-based and experimental techniques provide an holistic approach to characterize the biomechanical behaviour of teeth with both unrestored and restored NCCLs.

Key words: finite element analysis, fracture resistance test, non carious cervical lesion, premolar teeth, strain gauge test

Introduction

Non-carious cervical lesions (NCCLs) have a multifactorial origin, with the proposed predisposing factors being stress (abfraction), mechanical wear (from toothbrush/dentifrice abrasion) and biocorrosion (chemical degradation).[1] Computer modelling of the biomechanical behaviour of NCCLs using finite element analysis (FEA) indicates that cuspal flexure from heavy occlusal loading generates tensile forces at the cervical region of teeth, leading to microcrack initiation and propagation.[2-6] However, clinical findings of weak associations between occurrences of NCCLs and occlusal tooth wear, and anthropological findings of an absence of NCCLs in heavily worn pre-contemporary dentitions, raise doubts about the validity of the abfraction hypothesis.[7-9] Although FEA has limited predictive value in determining how NCCLs are formed, it is still a useful model to understand the biomechanical behaviour of both restored and unrestored teeth. For example, oblique occlusal loading generates greater stress at the tip of NCCLs than vertical loading, and restoration of NCCLs with a resin composite dissipates the stress.[10]

As there are inherent limitations with FEA, experimental data on stress distribution and fracture behaviour are crucial in gaining an overall understanding of biomechanical behaviour of heavily restored and endodontically treated teeth.[11-13] Fracture resistance tests yield information on the flexural properties of teeth but these tests are destructive in nature and do not provide information about stress-induced strain (deformation) behaviour leading up to the fracture. This crucial piece of information can be obtained from a combined assessment of both strain gauge testing[13,14] and FEA.[13,15,16] Previous studies have used a combined assessment of strain gauge testing and FEA to determine the risk of tooth fracture associated with resin composite veneers and endodontic restorations.[12,13,17-20] A combined assessment of the FEA, strain gauge test and fracture resistance test has been used in a handful of studies to investigate the biomechanical behaviour of endodontically treated teeth repaired with occlusal-proximal restorations, post cores and crowns.[12,21-23] Such information has the potential to improve the understanding of the biomechanical behaviour of coronal tooth structure compromised by NCCLs and carious lesions, as well as to assist in 'virtual prototyping' of restored teeth.[24]

The aim of this study was to analyze the biomechanical behavior of NCCLs in mandibular premolar teeth as a function of their size, restorative status and the direction of occlusal loading, using a combined assessment of FEA, strain gauge testing and fracture resistance testing.

Materials and Methods

Study design

The biomechanical behaviour of NCCLs under occlusal loading, as a function of their size and restorative status, was assessed using strain gauge tests and FEA in a longitudinal design, as well as fracture resistance tests in a cross-sectional design. Fracture resistance testing could not be modelled using a longitudinal design because the fractures rendered the

specimens inappropriate for retesting. Occlusal loads were applied to the buccal cusps of premolar teeth separately on the outer slope (for outer loading) and the inner slope (for inner loading).

For the strain gauge analysis, stress-induced micro-strain data were collected from 10 teeth at five different stages of NCCL development in a longitudinal design: (i) healthy (H) teeth at baseline, (ii) after each of the three stages of NCCL preparation (on the same teeth) by cutting 'V' notches at depths of 0.5 mm [i.e. small (L0.5) lesion], 1.0 mm [i.e. medium (L1.0) lesion], and then 1.5 mm [i.e. large (L1.5) lesion], and (iii) after restoration of large lesions with resin composite [i.e. restored (LR) lesion]. Strain gauges were placed close to the vicinity of the NCCLs to measure micro-strain values.

The five stages of strain gauge testing were also simulated using FEA to calculate stress-induced micro-strain values in different regions of the NCCLs. For fracture resistance testing, 42 premolar teeth were selected and tested for a combination of two variables: (i) two loading directions (i.e. outer and inner loading) and (ii) three states of NCCLs (including no NCCL/ healthy (H) teeth; large (L1.5) lesions; and restored (LR) lesions) [i.e. n = 7 per group × (2 × 3) groups].

Sample preparation

Fifty-two sound, single-rooted human mandibular premolar teeth of similar dimensions, and free of cracks and defects, were collected from patients aged between 28-30 years, who had attended the Dental Hospital of Federal University, Uberlandia, Brazil. The teeth wear stored in distilled water at 37 degrees Celsius for no longer than 3 months before experimentation, as described previously.[13] The teeth had been extracted as part of periodontal and orthodontic treatment with the consent of patients and approval from the Ethics Committee (#092/2010). The tooth size and shape were standardized by including teeth with normal occlusal morphology that fell within a deviation of ± 5% from the overall mean values for both

the bucco-lingual and mesio-distal widths. The teeth were cleaned with periodontal curettes, followed by prophylaxis with pumice-stone and water before being mounted in a polystyrene resin base. The periodontal ligament was simulated for strain gauge and fracture resistance testing by incorporating a thin layer of polyether (Impregum F, 3M-ESPE, St. Paul, MN, USA) between the roots of premolar teeth and the polystyrene base.[25]

NCCLs were prepared for strain gauge and fracture resistance testing on the buccal surfaces of premolar teeth at the cemento-enamel junction with a diamond bur (#3118 with grit size 50-70 µm and ISO number for flame shape 023; KG Sorensen, Barueri, São Paulo, Brazil) fitted in a high-speed handpiece (KaVo do Brasil Ltda, Joinville, SC,Brazil) that was mounted in a custom-made standardized preparation machine (Federal University of Uberlandia, Uberlandia, Minas Gerais, Brazil). The bur was capable of moving vertically and horizontally in increments of 3 µm with the aid of a micrometer (Mitutoyo, Tokyo, Japan), with an accuracy of 0.1 mm in the x-, y- and z-axes.

Restoration of deep lesions involved tooth preparation by etching with 37% phosphoric acid (3M ESPE, Minnesota, St Paul, USA) for 15 seconds, followed by washing with water for 15 seconds. Two layers of a 1-bottle adhesive system (Single Bond 2, 3M ESPE, Minnesota, St Paul, USA) were applied at an interval of 20 seconds before being light-cured for 20 seconds with a halogen source with an intensity of 800 mW/cm^2 (XL 3000, 3M ESPE, Minnesota, St Paul, USA). Then, a resin nanocomposite (Filtek XT, shade A3, Z350,3M ESPE, Minnesota, St Paul, USA) was placed in a single increment and light-cured for further 40 seconds.

Strain gauge testing

Two strain gauges (PA-06-060BG-350L; Excel Sensores, São Paulo, Brazil) were bonded to each tooth with a cyanoacrylate adhesive (Super Bonder; Loctite, São Paulo, Brazil), with wires connected to a data acquisition device (ADS0500IP; Lynx Tecnologia Eletronica Ltda.,

São Paulo, Brazil). One gauge was placed on the buccal surface of the tooth and the other on the mesial surface as shown in Fig. 1A. Each gauge consisted of a grid with an area of 1 mm x 2 mm and had an electrical resistance of 120 Ω.[12]

The gauge factor, referring to the proportional constant between electrical resistance variation and strain, was 2.12. In addition, the effect of thermal drifts on micro-strain values was calculated on a separate healthy tooth from the two strain gauges in the absence of occlusal loading. This allowed compensation of thermal drift to be made when calculating the micro-strain values from occlusal loading.[12] Vertical load was applied on the inner and outer surfaces of the buccal cusp of each specimen (Fig. 1B and C) with a metallic-wedge-load device (tip) at a speed of 0.5 mm/min to a maximum of 100 N in a mechanical testing machine (EMIC DL 2000; EMIC Equipamentos e Sistemas de Ensaio Ltda., São José dos Pinhais, Brazil).

Finite element analysis

Ten three-dimensional (3D) FEA models were created, representing five different experimental groups for both outer and inner loading. An extracted, intact human mandibular premolar was selected and the external contours of whole tooth (including the coronal and root surfaces), dentino-enamel junction and pulp chamber were generated using the Computer Assisted Design (CAD) software (Rhino3D 4.0, Rhinoceros, USA). The external contour of the whole tooth was generated by scanning it with a contact profilometer (MDX-40, Roland Co, Osaka, Japan). Then, the root surface was covered with utility wax, and the crown (enamel) was dipped in 10% hydrochloric acid solution for 10 min, before the remaining tooth structure (including the exposed dentino-enamel junction and the intact root surface) was rescanned as described previously.[26,27] Finally, the tooth was sectioned longitudinally using a precision saw and the contours of the pulp chamber on both sections were rescanned.

All digital files of the surface contours were exported in the *STL (stereolithographic) format to generate the 3D model for FEA using the CAD software. The final 3D FEA model contained the external and internal contours of enamel, dentine, pulp, polyether and polystyrene cylinder (Fig. 2A). These contours allowed construction of the non-uniform rational bezier spline (NURBS) surfaces and solids to create a three-dimensional model of a healthy tooth (Fig. 2B). The contours were created by point and line association using polyline module of CAD software. The unrestored NCCLs and the deep, restored NCCL were modelled by performing Boolean operations and the data were exported to the biomechanical analysis software ANSYS 12.0 (Ansys Workbench 12.0.1, PA, EUA) using the STEP format before further processing.

The pre-processing step comprised volume definition, data importation on mechanical properties of tooth structure, and mesh creation of each structure and boundary conditions. The processing step essentially involved calculation of stress values at different parts of the NCCLs. The post-processing step involved analysis of stress distribution inside and around the NCCLs. Solid quadratic tetrahedral elements with 10 nodes were used to simulate the mechanical properties of each structure described in the literature[12,28-30] (Table 1). The contours of the tooth surfaces and the supporting structures (Fig. 2C) were meshed with controlled and connected elements. After conducting a conversion mesh test, 0.3mm element nodal size was used for all solids except for polyether (0.2mm) and polystyrene resin (0.5mm). Specific mesh contact was created to improve the congruence and connectivity between the solids (Fig. 2D). The pulp tissue, polyether, polystyrene resin and resin composite were modelled in the FEA as elastic, isotropic and homogenous materials, whereas the enamel and dentine were assumed to be orthotropic (Table 1). A perfect bond was assumed when creating meshes between the resin composite and the tooth structure in the deep lesion.

A 100 N load was applied on the outer and inner slopes of the buccal cusp in the 3D model generated by the CAD Software (Fig. 2E and 2F) in accordance with the parameters described for the strain gauge testing.[3] The surfaces at the side and the base of the polystyrene cylinder were restricted in all degrees of freedom (Fig. 2E and 2F). The magnitude of the von Mises stress (Fig. 2G) and the maximum principal stress ($\sigma1$) (Fig. 2H) were calculated for all the five models. Three points were chosen for stress analysis in each NCCL, including its upper wall (UW), apex (A) and the lower wall (LW).

Fracture resistance testing

Fracture resistance testing was performed in a mechanical testing machine (EMIC DL 2000; EMIC São José dos Pinhais, Brazil) mounted to a wedge-shaped metallic device (tip) that applied loads on the outer and inner parts of the buccal cusps of premolar teeth at a cross-head speed of 0.5 mm/min until they fractured. Fracture patterns were examined under a stereomicroscope and categorized into four types: (i) Type I - a conservative fracture involving a small portion of the buccal cusp, (ii) Type II - a conservative fracture involving a small portion of the lingual cusp, (iii) Type III - a large fracture involving the base of the NCCL and extending above or at the level of the polysterene, and (iv) Type IV - a severe root and crown fracture extending below the polysterene (Fig. 3).

Statistical analysis

Statistical analysis was performed using the SPSS 13.0 software. The Shapiro-Wilk's test showed normal distribution and the Levene's test showed equal error variance of the dependent variable between the groups. Two-way analysis of variance (2x5) and Tukey HSD post hoc tests were conducted to determine (i) whether there were significant differences in the mean stress-induced micro-strain values between stages of NCCL preparation and loading directions, and (ii) whether there were significant differences in the

mean fracture resistance values between lesion size and loading directions. Statistical significance was set at the 0.05 probability level.

Results

Strain gauge testing

There were no significant differences between the micro-strain values of buccal and mesial strain gauges, so the data were pooled for further analysis. The means and standard deviations for micro-strain values are presented in Table 2. Two-way ANOVA confirmed significant effects of loading direction and lesion size on micro-strain values ($p<0.05$). The large (L1.5) lesions displayed highest mean micro-strain values and Tukey HSD test showed significant differences with the other groups for both loading directions ($p<0.05$). There were no significant differences in micro-strain values between healthy (H) specimens and other lesions (i.e. L0.5, L1.0 and LR lesions) for either outer or inner loading. The micro-strain values for outer loading were greater than those for inner loading for all groups ($p<0.05$) (Table 2).

Finite element analysis

The von Mises analysis showed that there was a direct relationship between NCCL size and stress concentration for both loading directions, with the highest stress concentration occurring at the apices of the NCCLs (Figs. 4 and 5). The results of the maximum principal stress analysis indicated that inner loading generated high tensile stress around the cemento-enamel junction on the contralateral side of loading (Fig. 6). Outer loading generated high tensile stress around the cemento-enamel junction on the same side of healthy and restored teeth (including resin composite and tooth surface interface in restored teeth), and around the buccal pulp horns of all teeth (including healthy teeth as well as unrestored and restored lesions) (Fig. 6). Stress distribution was highest around the apices

of NCCLs, with compressive stresses being generated from inner loading (-12.2 MPa in L0.5, -17.8 MPa in L1.0 and -19.2 MPa in L1.5; negative values indicating compressive stress) and tensile stresses being generated from outer loading (42.5 MPa in L0.5, 55.4 MPa in L1.0 and 59.6 MPa in L1.5; positive values indicating tensile stress) (Fig. 7). The patterns of stress concentration in LR lesions were similar to those of healthy teeth, but the magnitudes of tensile stress from both loading directions were lower in the former than the latter.

Fracture resistance testing

The mean fracture resistance values and standard deviations for the three different groups are presented in Table 3. Two-way ANOVA showed significant effects of NCCL type and loading directions on fracture resistance ($p<0.05$). Tukey test showed that the fracture resistance values were significantly greater for inner loading compared with outer loading, controlling for NCCL type ($p<0.05$). Large (L1.5) lesions displayed significantly lower fracture resistance values compared with healthy (H) teeth ($p<0.05$), but restored (LR) lesions displayed a significant recovery in fracture resistance ($p<0.05$). The distributions of fracture patterns are illustrated in Fig. 8.

Superficial (sum of Types I and Type II) fractures occurred frequently in healthy (H)

teeth for both loading directions, whereas deep (Type III) fractures occurred commonly

in deep (L1.5) lesions. Restoration of NCCLs resulted in the occurrence of the majority

of deep (Type III) fractures in LR lesions for inner loading, but more superficial (Type II) fractures from outer loading (Fig. 8).

Discussion

Experimental methods (such as strain gauge and testing and fracture resistance tesing) and computer simulated modelling (including finite element analysis) have different scopes and they yield data on different aspects of the mechanical properties of teeth. Specifically, these

properties relate to tensile stress generation in NCCLs, stress-induced strain and subsequent risk of fracture of the tooth structure from both outer loading (simulating lateral excursion) and inner loading (simulating clenching) in sound and restored forms.

Our findings of the strain gauge testing show similar patterns of stress distribution between healthy teeth and deep NCCL restored with resin composite. Clinically, resin composites and glass ionomer cements are most commonly used materials to restore NCCLs. Previous reports indicate high retention rates in NCCLs for etch-and-rinse resin composites (78-88% in 13 years[31]) and self-etch resin composites (90% in 3 years[32]). However, van Dijken and Pallesen[33] reported higher annual failure rates of 2.8-13.0% for four differetnt types of commercially available etch-and-rinse resin composites and 4.4% for a self-etch resin composite over 13 years, with lowest annual failure rates of 2.7% for glass ionomer cements. Burrow and Tyas have also reported the highest retention rate of 97% for glass ionomer cements compared with 90% for self-etching resin composites and 77% for etch-and-rinse resin composites over 3 year,[34] Eventually, bond degradation will occur at a varying degrees at the adhesive interface, and tensile stress concentration in large restored NCCLs (Fig. 6) will increase the likelihood of marginal leakage and adhesive failure. These findings point to the need to develop new, more stable and durable adhesive restorative materials than those currently available in order to restore the structural integrity and biomechanical function.[13,16,24]

Our findings of the FEA indicate that the presence of NCCLs, even as shallow as 0.5 mm, promotes stress concentration around the cervical region, with the magnitude of stress increasing with lesion size (Figs. 4 - 7). Both outer and inner occlusal loading generated higher stresses at the apex of the NCCL than on its upper and lower walls, indicating that the presence of the lesion could influence future lesion progression (Figs. 4 and 6).

The results of fracture resistance testing in the present study show that the presence of NCCLs alters the fracture patterns for both outer and inner loading. It is not evident from current findings which of the two occlusal loading forces is primarily responsible for crack propagation around areas of stress concentration (Figs. 4 and 5) that led to observations made during fracture resistance testing (Fig. 8). Fractographic analysis involving assessment of hackle lines that was used in the identification of the sites of crack initiation, propagation and termination in ceramic crowns[35,36] may assist in determining how occlusal loading gives rise to crack propagation in teeth. Furthermore, restoration of NCCLs significantly improved fracture resistance, almost to that of healthy teeth, irrespective of loading direction (Table 3). This is probably due to elimination of the 'sharp', wedge-shaped apex after restoration with a resin composite (with elastic modulus similar to dentine), resulting in even distribution of occlusal loads. Our previous studies have also indicated that NCCLs with sharp, acute angles display greater stress concentration at the apex than those with rounded apices,[10] and that the resin composite restorations result in similar distribution of stress in different types of NCCLs similar to sound teeth.[37]

The findings of the present study need to be interpreted with some caution. One of the limitations was that the study design did not allow the associations between stress concentration and crack initiation and propagation to be assessed. Consequently, it needs to be emphasized that the observed fracture patterns do not relate to the abfraction hypothesis. There were also the limitations of static loading and the assumption of homogeneity of the modelled structures in the FEA, that were partially overcome by the additional experimental techniques applied to investigate stress distribution (at relatively lower loads) and fracture occurrences (at relatively higher loads). Further research is needed to elucidate the fundamentals of fracture mechanics involved with crack initiation and propagation. This will require application of state-of-the-art micro-computed tomography imaging with sub-micron resolution to generate 3D FEA models.

It was outside the scope of the present study to control the variations in mineral content and dentine sclerosis between teeth because these techniques would have required invasive physical and mechanical testing, but technological advancements in 3D imaging systems could allow acquision of these data non-destructively and efficiently to enable these factors to be controlled in future studies. The sensitivity of the strain gauge testing also needs to be improved. It is also desirable to test the effect of outer loading closer to the proximity of the NCCLs, so that tensile forces are applied closer to the restoration/ tooth interface. Future work is also needed to incorporate the effects of reduced periodontal support on the biomechanical behavior of teeth when restored with new composite and glass ionomer cement products.

Conclusions

A combined assessment of findings from virtual 3D and experimental models have provided new insights into the mechanisms of stress distribution around NCCLs. Greater depth of NCCLs is associated with increased magnitude and extent of stress concentration. Loading on the outer slope of the buccal cusps of mandibular premolars inceased the chances of fracture compared with inner loading. Restoration with a resin composite improved structural integrity and biomechanical function around NCCLs almost to the levels of healthy teeth for loading in both directions.

References

1. Grippo JO, Simring M, Coleman TA. Abfraction, abrasion, biocorrosion, and the enigma of noncarious cervical lesions: a 20-year perspective. J Esthet Restor Dent 2012;24:10-23.
2. Lee WC, Eakle WS. Possible role of tensile stress in the etiology of cervical erosive lesions of teeth. J Prosthet Dent 1984;52:374-380.

3. Rees JS. The effect of variation in occlusal loading on the development of abfraction lesions: a finite element study. J Oral Rehabil 2002;29:188-193.

4. Rees JS, Hammadeh M, Jagger DC. Abfraction lesion formation in maxillary incisors, canines and premolars: a finite element study. Eur J Oral Sci 2003;111:149-154.

5. Rees JS, Hammadeh M. Undermining of enamel as a mechanism of abfraction lesion formation: a finite element study. Eur J Oral Sci 2004;112:347-352.

6. Rees JS. The role of cuspal flexure in the development of abfraction lesions: a finite element study. Eur J Oral Sci 1998;106:1028-1032.

7. Bernhardt O, Gesch D, Schwahn C, *et al.* Epidemiological evaluation of the multifactorial aetiology of abfractions. J Oral Rehabil 2006;33:17-25.

8. Michael JA, Townsend GC, Greenwood LF, Kaidonis JA. Abfraction: separating fact from fiction. Aust Dent J 2009;54:2-8.

9. Nguyen C, Ranjitkar S, Kaidonis JA, Townsend GC. A qualitative assessment of non-carious cervical lesions in extracted human teeth. Aust Dent J 2008;53:46-51.

10. Soares PV, Santos-Filho PC, Soares CJ, *et al.* Non-carious cervical lesions: influence of morphology and load type on biomechanical behaviour of maxillary incisors. Aust Dent J 2013;58:306-314.

11. Soares CJ, Martins LR, Fonseca RB, Correr-Sobrinho L, Fernandes Neto AJ. Influence of cavity preparation design on fracture resistance of posterior Leucite-reinforced ceramic restorations. J Prosthet Dent 2006;95:421-429.

12. Soares PV, Santos-Filho PC, Gomide HA, Araujo CA, Martins LR, Soares CJ. Influence of restorative technique on the biomechanical behavior of endodontically treated maxillary premolars. Part II: strain measurement and stress distribution. J Prosthet Dent 2008;99:114-122.

13. Soares PV, Santos-Filho PC, Martins LR, Soares CJ. Influence of restorative technique on the biomechanical behavior of endodontically treated maxillary premolars. Part I: fracture resistance and fracture mode. J Prosthet Dent 2008;99:30-37.

14. Ausiello P, De Gee AJ, Rengo S, Davidson CL. Fracture resistance of endodontically-treated premolars adhesively restored. Am J Dent 1997;10:237-241.

15. Benazzi S, Grosse IR, Gruppioni G, Weber GW, Kullmer O. Comparison of occlusal loading conditions in a lower second premolar using three-dimensional finite element analysis. Clin Oral Investig 2014;18:369-375.

16. Lin CL, Chang CH, Ko CC. Multifactorial analysis of an MOD restored human premolar using auto-mesh finite element approach. J Oral Rehabil 2001;28:576-585.

17. Reeh ES, Messer HH, Douglas WH. Reduction in tooth stiffness as a result of endodontic and restorative procedures. J Endod 1989;15:512-516.

18. Reeh ES, Ross GK. Tooth stiffness with composite veneers: a strain gauge and finite element evaluation. Dent Mater 1994;10:247-252.

19. Santana FR, Castro CG, Simamoto-Junior PC*, et al.* Influence of post system and remaining coronal tooth tissue on biomechanical behaviour of root filled molar teeth. Int Endod J 2011;44:386-394.

20. Santos-Filho PC, Castro CG, Silva GR, Campos RE, Soares CJ. Effects of post system and length on the strain and fracture resistance of root filled bovine teeth. Int Endod J 2008;41:493-501.

21. Santos-Filho PC, Veríssimo C, Soares PV, *et al.* Influence of ferrule, post system, and length on biomechanical behavior of endodontically treated anterior teeth. J Endod 2014;40:119-123.

22. Raposo LH, Silva GR, Santos-Filho PC, *et al.*Effect of anti-rotation devices on biomechanical behaviour of teeth restored with cast post-and-cores. Int Endod J 2010;43:681-191.

23. Verissimo C, Simamoto Junior PC, Soares CJ, Noritomi PY, Santos-Filho PC. Effect of the crown, post, and remaining coronal dentin on the biomechanical behavior of endodontically treated maxillary central incisors. J Prosthet Dent 2014;111:234-246.

24. Ichim I, Li Q, Loughran J, Swain MV, Kieser J. Restoration of non-carious cervical lesions Part I. Modelling of restorative fracture. Dent Mater 2007;23:1553-1561.

25. Soares CJ, Pizi EC, Fonseca RB, Martins LR. Influence of root embedment material and periodontal ligament simulation on fracture resistance tests. Braz Oral Res 2005;19:11-16.

26. Soares PV, Souza LV, Verissimo C*, et al.* Effect of root morphology on biomechanical behaviour of premolars associated with abfraction lesions and different loading types. J Oral Rehabil 2014;41:108-114.

27. Soares PV, Milito GA, Pereira FA*, et al.* Rapid prototyping and 3D-virtual models for operative dentistry education in Brazil. J Dent Educ 2013;77:358-363.

28. Miura J, Maeda Y, Nakai H, Zako M. Multiscale analysis of stress distribution in teeth under applied forces. Dent Mater 2009;25:67-73.

29. Toparli M. Stress analysis in a post-restored tooth utilizing the finite element method. J Oral Rehabil 2003;30:470-476.

30. Shinya A, Yokoyama D, Lassila LV, Vallittu PK. Three-dimensional finite element analysis of metal and FRC adhesive fixed dental prostheses. J Adhes Dent 2008;10:365-371.

31. Peumans M, De Munck J, Van Landuyt KL, Poitevin A, Lambrechts P, Van Meerbeek B. A 13-year clinical evaluation of two three-step etch-and-rinse adhesives in non-carious class-V lesions. Clin Oral Investig 2012;16:129-137.

32. Burrow MF, Tyas MJ. Comparison of two all-in-one adhesives bonded to non-carious cervical lesions--results at 3 years. Clin Oral Investig 2012;16:1089-1094.

33. van Dijken JW, Pallesen U. Long-term dentin retention of etch-and-rinse and self-etch adhesives and a resin-modified glass ionomer cement in non-carious cervical lesions. Dent Mater 2008;24:915-922.

34. Burrow MF, Tyas MJ. Clinical evaluation of three adhesive systems for the restoration of non-carious cervical lesions. Oper Dent 2007;32:11-15.

35. Oilo M, Hardang AD, Ulsund AH, Gjerdet NR. Fractographic features of glass-ceramic and zirconia-based dental restorations fractures during clinical function. Eur J Oral Sci 2014;122:228-244.

36. Oilo M, Kvam K, Gjerdet NR. Simulation of clinical features for three different all ceramic crowns. Eur J Oral Sci 2014;122:245-250.

37 Soares PV, Machado AC, Zeola LF, Souza PG, Galvão AM, Montes TC, Pereira AG, Reis BR, Coleman TA, Grippo JO. Loading and composite restoration assessment of various non-carious cervical lesions morphologies - 3D finite element analysis. Aust Dent J 2015;60:309-316.

Figure Legends

Fig. 1 Strain gauge testing around the cervical regions of mandibular premolar teeth, showing: (a) strain gauge positions; (b) inner load application; and (c) outer load application.

Fig. 2 Three-dimensional finite element model generation. (a) external and internal contours that were traced by computer-aided design software; (b) volumes of each structure in Rhinoceros software; (c) visualization of dental tissues and structures in ANSYS software; (d) zoom-in of meshes of all structures; (e) inner load application and displacement restriction on the blue area; (f) outer load application and displacement restriction on the blue area; (g) von Mises stress distribution (MPa), and (h) maximum principal stress (MPa) distribution.

Fig. 3 Fracture patterns identified from fracture resistance testing for both outer and inner loading on mandibular premolar teeth: (a) Type I - a conservative fracture involving a small portion of the buccal cusp; (b) Type II - a conservative fracture involving a small portion of the lingual cusp; (c) Type III - a large fracture involving the base of the NCCL and extending above or at the level of the polysterene; and (d) Type IV - a severe root and crown fracture extending below the polysterene.

Fig. 4 von Mises stress distribution (in MPa) in finite element analysis of five different types of non-carious cervical lesions under both outer and inner occlusal loading (blue = 0; red = 30MPa).

Fig. 5 von Mises stress values (in MPa) obtained from finite element analysis of five different types of non-carious cervical lesions from the outer and inner occlusal loading at the upper wall (UW), the apex (A) and the lower wall (LW) of each lesion.

Fig. 6 Maximum principal stress distribution (in MPa) in finite element analysis of five different types of non-carious cervical lesions (NCCLs) under both outer and inner occlusal loading. The left images represent 2D sagittal sections of each tooth, with or without NCCLs, and the right images (insets) show 3D images of the NCCL region around the cemento-enamel junction in a bucco-proximal axis (at 5× magnification). Positive values represent tensile stress (red = 20 MPa) and negative values represent compressive stress (blue = 15 MPa).

Fig. 7 Maximum principal stress values (in MPa) obtained from finite element analysis within three specific areas of non-carious cervial lesions, including the upper wall (UW), the apex (A) and the lower wall (LW) of each lesion, from both outer and inner occlusal loading.

Fig. 8 Fracture patterns observed at the completion of fracture resistance testing in Healthy (H) teeth; large, unrestored (L1.5) lesions; and large restored (LR) lesions. The percentages represent the frequencies of occurrence of different fractures from outer and inner occlusal loading. The colored teeth in the background show von Mises stress distribution for different types of lesions as shown in Fig. 4.

Table 1. Mechanical properties used to construct three-dimensional finite element models of teeth. Enamel and dentine were assumed to be orthotropic structures and pulp, polyether, polystyrene resin and nanohybrid resin composite were assumed to be isotropic structures. The numbers in brackets indicate references from which the values for mechanical properties were derived.

Hard tissues	SAGITTAL PLANE	CORONAL PLANE	AXIAL PLANE
Orthotropic Structures [28]			
Elastic Modulus (GPa)			
Enamel	73,72	63,27	63,27
Dentin	17,07	5,61	5,61
Shear coefficient (GPa)			
Enamel	20,89	24,07	20,890
Dentin	1,700	6,00	1,70
Poisson Ratio (v)			
Enamel	0.23	0.45	0.23
Dentin	0.30	0.33	0.30
Isotropic Structures			
	Elastic Modulus (GPa)	Poisson Ratio (v)	
Pulp [29]	0.002	0.45	
Polyether [12]	0.050	0.45	
Polystyrene Resin [12]	13,7	0.30	
Resin nanocomposite [30]	22,0	0.27	

Table 2. Micro-strain values of different types of non-carious cervical lesions (NCCLs) for both outer and inner occlusal loading using a longitudinal assessment of mandibular premolar teeth (N = 10)

NCCL type	Inner loading†		Outer loading†	
	Mean	SD	Mean	SD
Healthy (H) teeth (i.e. no lesion)	527.9	224.8	722.8	300.0
Small (L0.5) lesions	634.0	236.9	744.0	192.3
Medium (L1.0) lesions	854.4	240.1	934.5	426.6
Large (L1.5) lesions*	1306.5	286.3	1486.0	361.4
Large restored (LR) lesions	651.9	259.1	790.4	244.2

*Tukey HSD test confirmed significantly greater mean micro-strain values in Large (L1.5) lesions compared with other leasions (i.e. Healthy teeth, smaller (L0.5 and L1.0) lesions and Large restored lesions), controlling for inner and outer loading (p<0.05)

†Tukey HSD test confirmed significantly greater mean micro-strain values for outer loading compared with inner loading, controlling for NCCL type (p<0.05)

Table 3. Mean fracture resistance (standard deviation) values of different types of non-carious cervical lesions (NCCLs) for both outer and inner occlusal loading

NCCL type	Inner loading†			Outer loading†		
	N	Mean	SD	N	Mean	SD
Healthy (H) teeth (i.e. no lesion)	7	1032.7	420.6	7	503.9	186.3
Large (L1.5) lesion*	7	641.4	157.5	7	249.6	99.5
Large restored (LR) lesion	7	903.4	361.9	7	352.3	146.3

*Tukey HSD test confirmed significantly greater mean micro-strain values in Large (L1.5) lesions compared with other lesions (i.e. Healthy teeth, smaller (L0.5 and L1.0) lesions and Large restored lesions) for inner load (p<0.05)

†Tukey HSD test confirmed significantly greater mean micro-strain values for outer loading compared with inner loading, controlling for NCCL type (p<0.05)
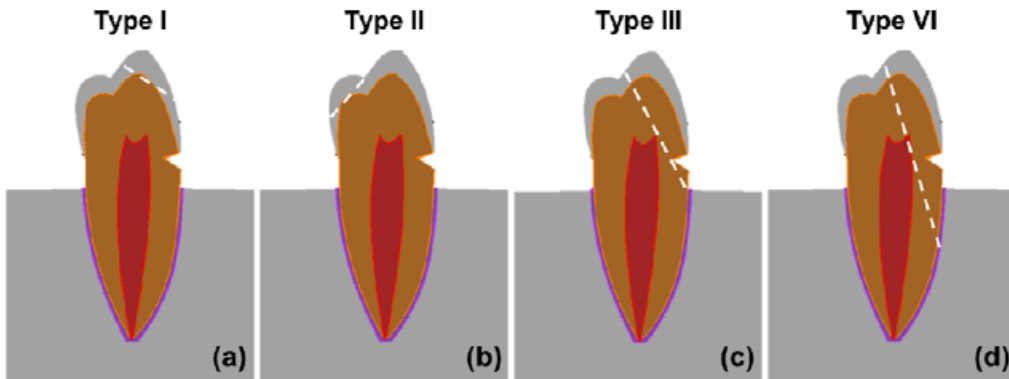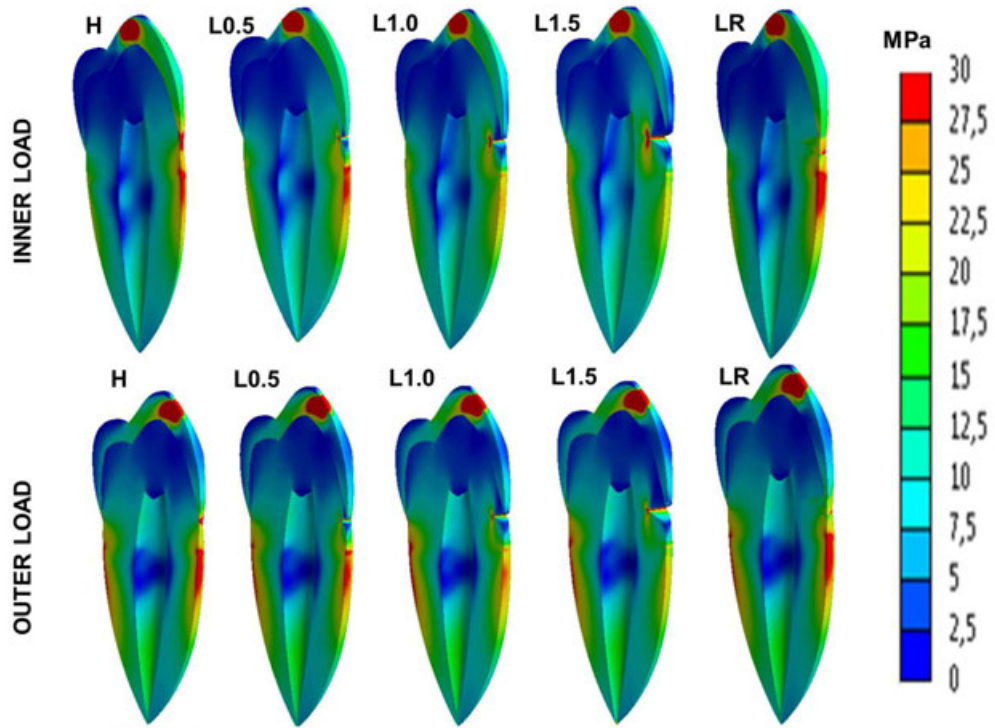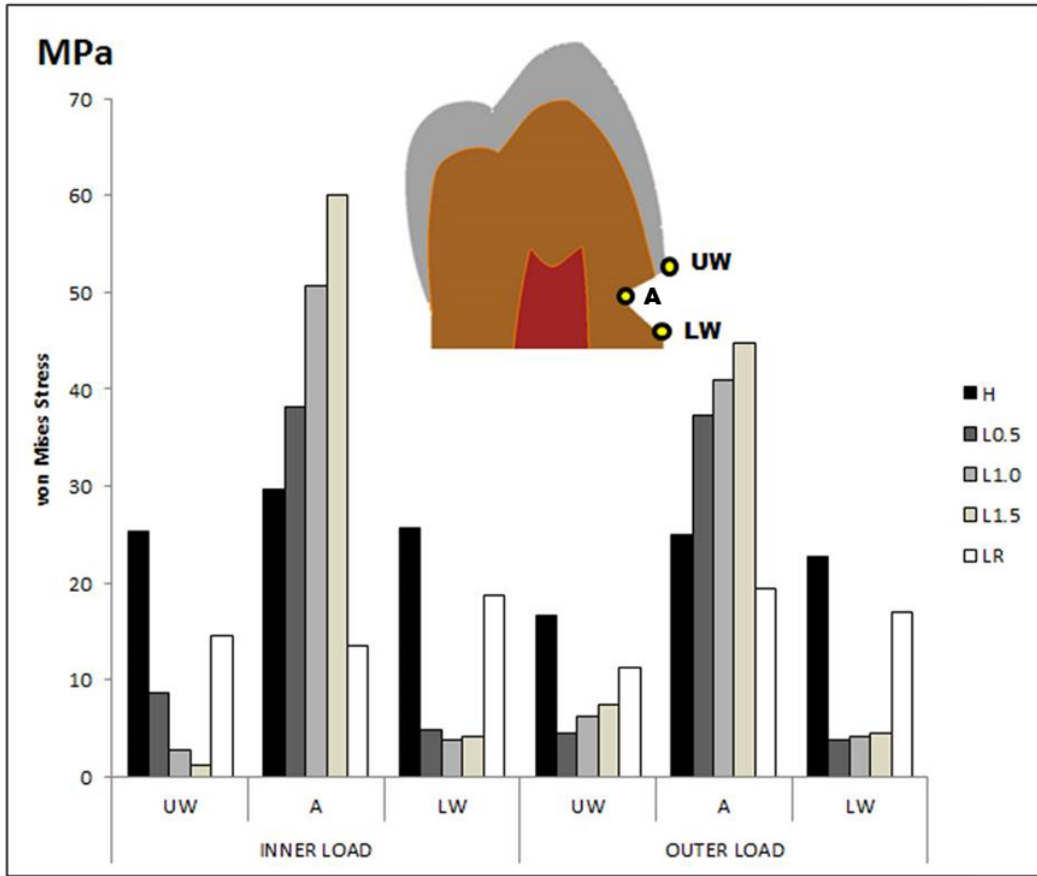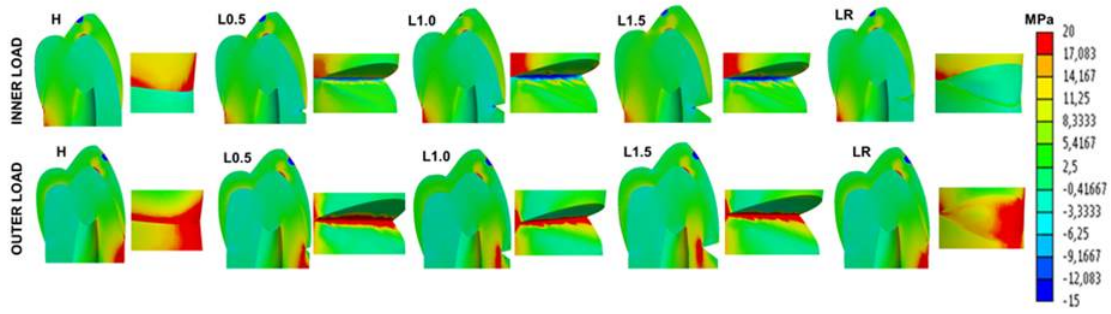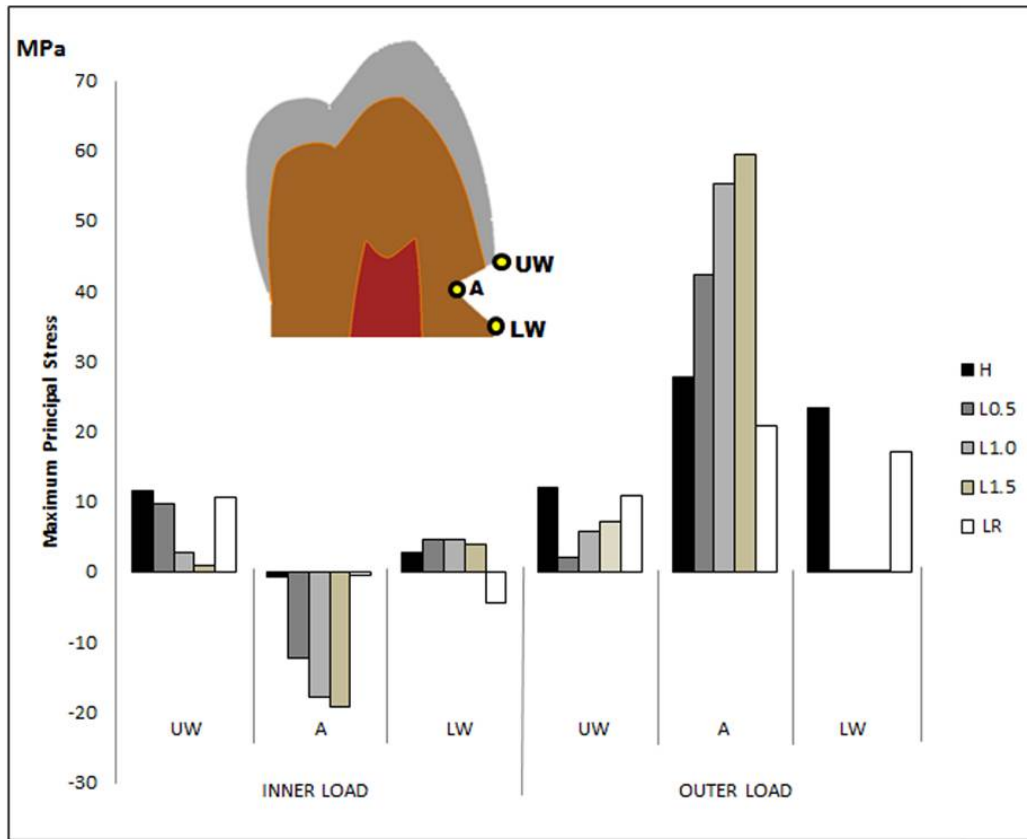
Figure 1
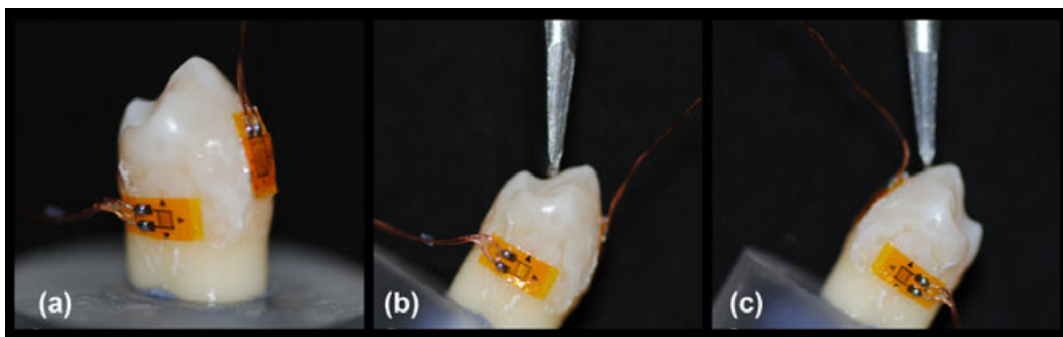
Figure 2
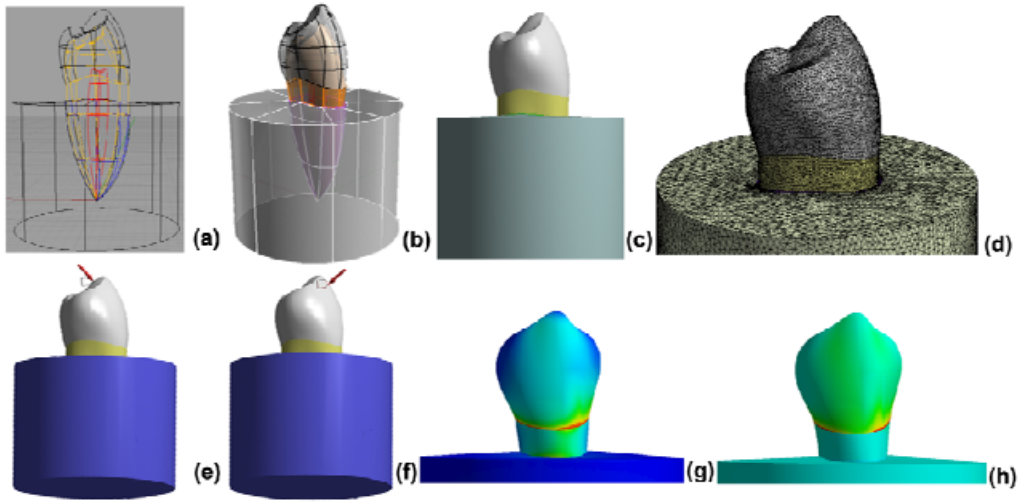
Figure 3

Figure 4

Figure 5

Figure 6

Figure 7

Figure 8